

Global Optimization for IRS-Assisted Wireless Communications: from Physics and Electromagnetic Perspectives

Xin Cheng, Yan Lin, Weiping Shi, Jiayu Li, Cunhua Pan, Feng Shu, and Jiangzhou Wang, *Fellow*, IEEE

Abstract—Intelligent reflecting surfaces (IRSs) are envisioned to be a disruptive wireless communication technique that is capable of reconfiguring the wireless propagation environment. In this paper, we study a far-field IRS-assisted multiple-input single-output (MISO) communication system operating in free space. To maximize the received power of the receiver from the physics and electromagnetic nature point of view, an optimization, including beamforming of the transmitter, phase shifts of the IRS, orientation and position of the IRS is formulated and solved. After exploiting the property of line-of-sight (LoS), we derive closed-form solutions of beamforming and phase shifts. For the non-trivial IRS position optimization problem in arbitrary three-dimensional space, a dimensional-reducing theory is proved, which is useful to reduce the complexity of search method. The simulation results show that the proposed closed-form beamforming and phase shifts are near-optimal solutions. Besides, the IRS significantly enhances the performance of the communication system when it is deployed at the optimal position.

Index Terms—Intelligent Reflecting Surface (IRS), multiple-input single-output (MISO), uniform linear array (ULA), closed-form beamforming and phase shifts, position optimization, millimeter wave communication.

I. INTRODUCTION

In recent years, wireless communication has witnessed great success in various aspects such as rate, stability and security. However, most of the existing techniques mainly rely on the transceiver design at both the transmitter and the receiver. The wireless propagation environment is left untouched. Unfortunately, the propagation loss and multi-path fading deteriorate the communication performance. Due to the rapid development of radio frequency (RF), micro electro-mechanical systems (MEMS) and metamaterial, a metasurface called intelligent reflecting surface (IRS) [1], [2] has attracted a lot of attention. In [3], a new wireless communication paradigm based on the concept of IRS was proposed, which can adaptively tune the propagation environment. The benefits and challenges were discussed in [4].

Xin Cheng, Yan Lin, Weiping Shi, Jiayu Li are with School of Electronic and Optical Engineering, Nanjing University of Science and Technology, Nanjing, 210094, China.

F. Shu is with the School of Information and Communication Engineering, Hainan University, Haikou 570228, China. and also with the School of Electronic and Optical Engineering, Nanjing University of Science and Technology, Nanjing 210094, China (e-mail: shufeng0101@163.com).

Cunhua Pan is with the School of Electronic Engineering and Computer Science, Queen Mary University of London, Mile End Road London E1 4NS, U.K. (e-mail: yongpeng.wu2016@gmail.com).

Jiangzhou Wang is with the School of Engineering and Digital Arts, University of Kent, Canterbury CT2 7NT, U.K. (e-mail: j.z.wang@kent.ac.uk).

An IRS is composed of an array of low-cost passive reflecting elements, each of which can be controlled by a control loop to re-engineer the electromagnetic wave (EM) including steering towards any desired direction full absorption, polarization manipulation. The EM programmed by many reflecting elements can be integrated constructively to induce remarkable effect. Unlike relay which requires active radio frequency (RF) chains, the IRS is passive because it does not adopt any active transmit module (e.g., power amplifier) [5]. Hence, the IRS is more energy efficient than the relay scheme.

Due to the above appealing features, IRS-assisted communication systems have been studied extensively. For example, by jointly designing beamforming of the transmitter and phase shifts of the IRS, the IRS-assisted system can achieve the same rate performance as an IRS-free massive multiple-input multiple-output (MIMO) system without using IRS with less power consumption [6]. The joint design of beamforming and phase shifts was also investigated in various communication scenarios. The contributions in [7]–[10] showed that the IRS offers performance improvement and coverage enhancement in the single-user multiple-input single-output (MISO) system. In downlink multi-user MISO case, the advantages of introducing IRSs in enhancing the cell-edge user performance were confirmed in [11]. Employing IRSs to wireless information and power transfer (SWIPT) system in multi-user MIMO scenarios was shown to beneficially enhance the system performance in terms of both the link quantity and the harvested power [12]. The advantages of introducing IRS were demonstrated in a secure multigroup multicast MISO communication system in [13]. To minimize the symbol error rate (MSER) of an IRS-assisted point-to-point multi-data-stream MIMO wireless communication system, the reflecting elements at the RIS and the precoder at the transmitter were alternately optimized in [14]. With the assistance of IRSs, secrecy communication rate i.e., physical layer security can be significantly improved [6], [15]. The work of [16] examined the performance gain achieved by deploying an IRS in covert communications. IRS was proposed to create friendly multipaths for directional modulation (DM) such that two confidential bit streams (CBSs) can be transmitted from Alice to Bob in [17]. The important theoretical performance like ergodic spectral efficiency, symbol error probability, and outage probability was analysed and optimized in [10], [11], [18]. The channel estimation in the IRS-assisted scenario was studied in [19], [20]. More realistic limits like discrete phase-shift and phase-dependent amplitude were considered in [21], [22]. The authors in [23]

proposed a reflecting modulation (RM) scheme for IRS-based communications, utilizing both the reflecting patterns and transmit signals to carry information.

However, the above papers applied simple mathematical models that regard the IRS reflecting elements as a diagonal matrix with phase shifts values, leading to relatively simplified algorithm designs and performance predictions. There are some existing works that have studied the physical and electromagnetic models of IRS in free space [24]–[26]. The responses of the IRSs to the radio waves were studied and based on this, physics and electromagnetic path loss models in free space was established. The works showed that the path loss model in near-field/far-field scenarios are of two kinds, depending on the distance between the IRS and the transmitter/receiver. In the far-field condition, the spherical wave generated by the transmitter can be approximately regarded as a plane wave [27]. Thus it is more tractable for theoretical analysis. The proposed free-space path loss model in [26], which is first validated through extensive simulation results, revealed the relationships between the free-space path loss of IRS-assisted wireless communications and the distances from the transmitter/receiver to the IRS, the size of the IRS, the near-field/far-field effects of the IRS, and the radiation patterns of antennas and unit cells. Moreover, the analytical model matches quite well with the experiments in a microwave anechoic. Therefore, we apply the tractable and reliable path loss model proposed in [26] to our work.

From the physics and electromagnetic point of view, how much performance gain can be brought in by IRS is an important question. In this paper, we consider a far-field IRS-assisted MISO wireless communication system in free space. To achieve the performance limit of this system, an optimization, including beamforming of the transmitter, phase shifts of the IRS and placement of the IRS, is addressed.

Our main contributions are summarized as follows:

- 1) The comprehensive optimization problem of far-field IRS-assisted wireless communication in free space, considering the physics and electromagnetic nature of IRS, is formulated. By exploiting the propagation property of electromagnetic wave in free space, under the principle of phase alignment and maximum ratio transmission, we derive closed-form solutions of beamforming and phase shifts to maximize the received power. Due to the extreme accuracy of the approximation technology, the closed-form solutions are near-optimal, verified in simulation part. Besides, it is found that the optimal orientation of IRS is just to perform specular reflection. Moreover, a design principle of manufacturing IRSs is provided to counteract the deteriorating path loss of high-frequency electromagnetic wave.
- 2) In order to reap full advantage brought by IRS, the problem of where to place an IRS in an arbitrary three-dimensional space is formulated and discussed. By excavating the quasi-convex property of the objective function, we demonstrate that the optimal position is always on the boundary of the two-dimensional area of interest. Then the theorem is naturally extended to arbitrary three-dimensional space. This work provides the

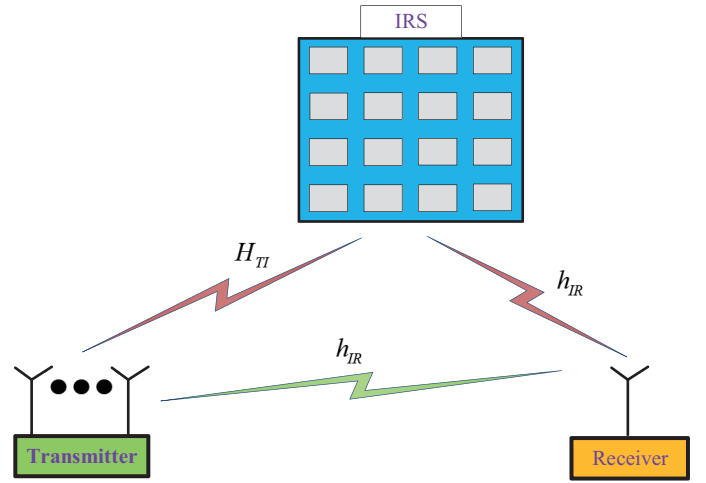


Fig. 1. Diagram of IRS-assisted wireless communication system.

theoretical basis of reducing the complexity of general search method by essentially reducing the dimension of the area of interesting. The simulation results show that the significant received power gain can be obtained after performing position optimization of the IRS.

The remainder of this paper is organized as follows. In Section II, we describe the system model of IRS-assisted wireless communication. After considering the physical and electromagnetic nature of the IRS, a joint optimization problem is formulated. We provide the closed-form beamforming and phase shifts, as well as the optimal orientation of the IRS in Section III. Subsequently, we discuss the performance gain brought by an IRS at the end of this section. Based on above, a reduced-dimension theory for applying search method to find the optimal position of the IRS is proved in Section IV. The proposed comprehensive scheme is numerically evaluated in Section V. Finally, we draw conclusions in Section VI.

Notations: Boldface lower case and upper case letters denote vectors and matrices, respectively. $(\cdot)^H$ denotes conjugate and transpose operation. $\mathbb{C}^{x \times y}$ denotes the space of $x \times y$ complex matrices. $\mathbb{E}\{\cdot\}$ represents expectation operation. $\|\cdot\|$ denotes 2-norm while $\|\cdot\|_F$ denotes Frobenius norm. $\text{diag}(\cdot)$ denotes a diagonal matrix whose diagonal elements are given by the corresponding vector.

II. SYSTEM MODEL AND PROBLEM FORMULATION

A. System Model

Consider a MISO wireless system where an IRS is deployed to assist in the communication from the transmitter of M antennas, forming uniform linear array (ULA), to a single-antenna user, as illustrated in Fig. 1. The symmetric and regular IRS consists of L reflecting elements with N_I rows and M_I columns. The length of the single reflecting element is denoted as d_x while d_y denotes the width of it. The received signal is the sum of the direct link and the IRS-assisted link. The distance between the transmit/receiver and the center of the IRS is far enough, so that the transmit/receiver is in far

field of the IRS. For simple notations, the IRS, the transmitter, and the receiver are denoted as I, T, and R, respectively.

The channel matrices from T to I, from T to R, and from I to R are denoted by $\mathbf{H}_{TI}^H \in \mathbb{C}^{L \times N}$, $\mathbf{h}_{IR}^H \in \mathbb{C}^{1 \times L}$ and $\mathbf{h}_{TR}^H \in \mathbb{C}^{1 \times N}$, respectively. Note that, in LoS, the channel element is mainly related to the position relationships of the communication parties. The element of matrix \mathbf{H}_{TI}^H at the p -th column and the q -th row can be written as $a_{TI,p,q} e^{j\theta_{TI,p,q}}$, which is determined by the distance from the p -th antenna of T to the q -th reflecting element. Similarly, the q -th column of \mathbf{h}_{IR}^H is represented as $a_{IR,q} e^{j\theta_{IR,q}}$ and the p -th column of \mathbf{h}_{TR}^H is denoted as $a_{TR,p} e^{j\theta_{TR,p}}$.

In this paper, it is assumed that the positions of T and R are fixed and known. Our goal is to maximize the received power at R by designing beamforming of T and phase shifts of I, as well as solving the IRS placement problem. After selecting a coordinate system and choosing the center point of the transmitter/receiver and the IRS as reference points, we represent the positions of T, I, and R by vector \mathbf{r}_T , \mathbf{r}_I , and \mathbf{r}_R respectively. When representing the position of the q -th reflecting element as $\mathbf{r}_{I,q}$, the centre point of the q -th reflecting element is chosen as the reference point. Similarly, $\mathbf{r}_{T,p}$ is used to denote the position of the p -th antenna of T. The position's relationship between the elements and the IRS can be represented by a function as $\mathbf{r}_{I,q} = f(\mathbf{r}_I, q)$. The function $f(\cdot)$ is determined by the placement mode of the IRS and the shape of it for a symmetric and regular IRS. Similarly, $\mathbf{r}_{T,p} = g(\mathbf{r}_T, p)$, g is a function determined by the direction of ULA and the antenna spacing Δd_T . Let $\Delta d_{T,p}$ denote the distance from the p -th antenna to the reference point of T, given by

$$\Delta d_{T,p} = \left(\frac{N+1}{2} - p \right) \Delta d_T, \quad p = 1 \cdots N. \quad (1)$$

The distance from the p -th antenna element to the q -th IRS reflecting element denoted by $d_{TI,p,q}$ can be expressed as

$$d_{TI,p,q} = |\mathbf{r}_{I,q} - \mathbf{r}_{T,p}|, \quad p = 1 \cdots N, \quad q = 1 \cdots L. \quad (2)$$

It should be noticed that the rule of numbering sequence for antennas of T or elements of IRS is flexible and has no impact on the final result.

The amplitude gain $a_{TI,p,q}$ in the channel is inversely proportional to $d_{TI,p,q}^2$, according to the propagation principle of electromagnetic wave. In far-field case, the distance and direction from different antenna elements to different IRS elements can be assumed the same when calculating amplitude gains, which means that all $a_{TI,p,q}$ can be assumed to be the same. Shown as following, this kind of approximation can be taken in all the channel matrices.

$$a_{TI,p,q} \approx a_{TI}, \quad a_{IR,q} \approx a_{IR}, \quad a_{TR,p} \approx a_{TR}. \quad (3)$$

We denote $a_{TI}a_{IR}$ as the final amplitude gain from the transmitter to the receiver through individual reflecting element of the IRS. Thus the channels above can be given by

$$\mathbf{H}_{TI}^H = a_{TI} \begin{bmatrix} e^{j\theta_{TI,1,1}} & \cdots & e^{j\theta_{TI,1,N}} \\ \vdots & \ddots & \vdots \\ e^{j\theta_{TI,L,1}} & \cdots & e^{j\theta_{TI,L,N}} \end{bmatrix}, \quad (4)$$

TABLE I
SOME PARAMETERS IN PHYSICS AND ELECTROMAGNETIC
IRS-ASSISTED PATH LOSS MODEL

Symbol	Definition
Z_0	The characteristic impedance of the air
G_t	Antenna gain of transmitter
G	Gain of the IRS
F	Normalized power radiation pattern
θ_t	The elevation angle from the reference point of the IRS to the transmitter
φ_t	The azimuth angle from the reference point of the IRS to the transmitter
θ_r	The elevation angle from the center of the IRS to the receiver
φ_r	The azimuth angle from the center of the IRS to the receiver
Γ	The reflection coefficient
A_t	The aperture of the transmitting antenna
A_r	The aperture of the receiving antenna

$$\mathbf{h}_{IR}^H = a_{IR} [e^{j\theta_{IR,1}}, \dots, e^{j\theta_{IR,L}}], \quad (5)$$

$$\mathbf{h}_{TR}^H = a_{TR} [e^{j\theta_{TR,1}}, \dots, e^{j\theta_{TR,N}}]. \quad (6)$$

In such a MISO system, the useful message x is sent from T to R, which is normalized such that $\mathbb{E}\{x^H x\} = 1$. Besides, they are multiplied by the beamforming vector $\mathbf{v} = (v_1 v_2 \cdots v_N)$ with the power limit P_t ($\mathbf{v}^H \mathbf{v} \leq P_t$). In order to combine with the physics path loss model hereinafter, P_t accounts for the signal power in the linear domain at unit distance. The phase-shift matrix of the IRS, representing the properties of the IRS, is denoted by $\Theta = \text{diag}(\theta) \in \mathbb{C}^{L \times L}$ with $\theta = [\theta_1, \theta_2, \dots, \theta_L]$. All the elements in θ satisfy the condition $\theta_i^H \theta_i = 1$, $i = 1, \dots, L$.

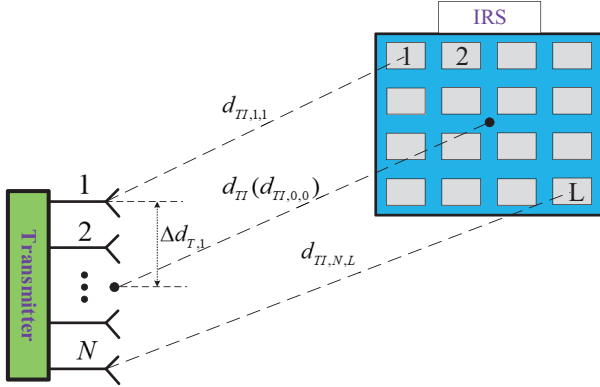
The power of the received signal, which is a sum of the direct link and the IRS-assisted link, can be expressed by

$$P_r = |(\mathbf{h}_{IR}^H \Theta \mathbf{H}_{TI}^H + \mathbf{h}_{TR}^H) \mathbf{v}|^2. \quad (7)$$

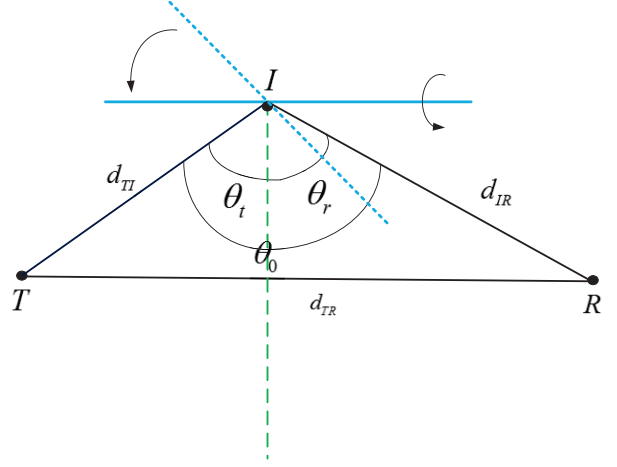
B. Physical and Electromagnetic Perspective

In this subsection, we shall express the amplitude gain and phase changes of the channels from physical and electromagnetic perspective. The parameters mentioned in this subsection are explained in Table I. Let us first concretize the amplitude gain from T to R through individual reflecting element, i.e., $a_{TI}a_{IR}$ is of first priority. Referring to the path loss model of far-field case described in [26], we obtain

$$\begin{aligned} a_{TI}a_{IR} &\triangleq a_{TIR} \\ &= \frac{\sqrt{2Z_0 P_t G_t G_d d_x d_y F(\theta_t, \varphi_t) F(\theta_r, \varphi_r) \Gamma^2 A_r}}{A_r 16\pi^2} d_{TI}^{-1} d_{IR}^{-1} \\ &= \frac{\sqrt{P_t}}{\sqrt{2Z_0 G_t G_d d_x d_y F(\theta_t, \varphi_t) F(\theta_r, \varphi_r) \Gamma^2}} d_{TI}^{-1} d_{IR}^{-1} \\ &\triangleq \delta_{TIR} d_{TI}^{-1} d_{IR}^{-1}. \end{aligned} \quad (8)$$



(a) Some notations mentioned in (12) and (18).



(b) Tuning an IRS at a fixed position.

Fig. 2. Notations

Similarly, the amplitude gain from direct link can be expressed as

$$a_{TR} = \frac{\sqrt{\frac{2Z_0 P_t G_t A_r}{A_r 4\pi}}}{\sqrt{P_t}} d_{TR}^{-1} = \sqrt{\frac{Z_0 G_t}{2\pi}} d_{TR}^{-1} \triangleq \delta_{TR} d_{TR}^{-1}. \quad (9)$$

Notice that normalized power radiation pattern of the IRS is denoted as $F(\theta_t, \varphi_t)F(\theta_r, \varphi_r)$. The general normalized power radiation pattern of a single reflecting element is in the form of

$$F(\theta_t, \varphi_t) = \begin{cases} \cos^k \theta_t & \theta_t \in [0, \frac{\pi}{2}], \varphi_t \in [0, 2\pi] \\ 0 & \theta_t \in (\frac{\pi}{2}, \pi], \varphi_t \in [0, 2\pi] \end{cases} \quad (10)$$

where $k \geq 0$. $F(\theta_r, \varphi_r)$ has the same structure. Thus, turning an IRS at a fixed position impacts the amplitude gain $a_{TI}a_{IR}$. Fig. 2(b) illustrates this problem. From above, the amplitude gain in the channel through IRS is essentially a function of the position of the IRS, denoted as \mathbf{r} and orientation of the IRS, denoted as ξ .

According to the principle of propagation of electromagnetic wave (EM), the phase change of the EM and the propagation distance satisfies

$$\theta_{TI,q,p} = \frac{2\pi}{\lambda} d_{TI,p,q}, \quad 1 \leq p \leq N, 1 \leq q \leq L. \quad (11)$$

where λ is the carrier wavelength. Because the size of the reflecting element and the antenna element separation is the same order or sub-order of the carrier wavelength, unlike amplitude gain, different phase changes cannot be assumed to be the same. However, similar to the MIMO model in free space [28], the phase change can be strictly approximated as

$$\begin{aligned} \theta_{TI,q,p} &\stackrel{a}{\approx} \frac{2\pi}{\lambda} \underbrace{(d_{TI,0,q} + \Delta d_{T,p} \cos \mu_{TI,q})}_{\bar{d}_{TI,q,p}} \\ &\stackrel{b}{\approx} \frac{2\pi}{\lambda} (d_{TI,0,q} + \Delta d_{T,p} \cos \mu_{TI}), \\ &\stackrel{c}{\approx} \frac{2\pi}{\lambda} (d_{TI} - \sin \theta_t \cos \varphi_t (m_q - \frac{M_I + 1}{2})d_x \\ &\quad - \sin \theta_t \sin \varphi_t (n_q - \frac{N_I + 1}{2})d_y \\ &\quad + (\frac{N + 1}{2} - p)\Delta d_T \cos \mu_{TI}), \end{aligned} \quad (12)$$

where d_{TI} denotes the distance from the reference point of antenna array to the reference point of IRS, μ_{TI} denotes the complement angle of the DOA of the IRS at the transmitter, m_q is the index number of columns of the q -th element and n_q is the index number of rows of the q -th element. Fig. 2a illustrates the above notations. It is worth mentioning that there are $\sin(\cdot)$ functions instead of $\cos(\cdot)$ functions in existing works [29], [30] due to the use of the supplementary angle. In more details, approximate equation (a) requires $d_{TI} \gg \Delta d_{T,p}$ and approximate equation (b) assumes that all DOAs of different elements in the IRS are the same, which requires $d_{TI} \gg \max_q \{d_{TI,0,q} - d_{TI}\}$. Besides approximate equation (c) requires $d_{TI} \gg \sqrt{m_q^2 d_x^2 + n_q^2 d_y^2}$, based on the formula (32) in [26].

Similarly, under the far-field condition, the following approximations are also written as

$$\theta_{IR,q} \approx \frac{2\pi}{\lambda} (d_{IR} - \sin \theta_r \cos \varphi_r (m_q - \frac{1}{2})d_x - \sin \theta_r \sin \varphi_r (n_q - \frac{1}{2})d_y). \quad (13)$$

$$\theta_{TR,p} \approx \frac{2\pi(d_{TR} + (\frac{N+1}{2} - p)\Delta d_T \cos \mu_{TR})}{\lambda}. \quad (14)$$

The far-field conditions for (12), (13) and (14) are summarized as follows

$$d_{TI} \gg N\Delta d_T, \quad (15a)$$

$$d_{TI} \gg L\sqrt{d_x^2 + d_y^2}, \quad (15b)$$

$$d_{IR} \gg L\sqrt{d_x^2 + d_y^2}, \quad (15c)$$

$$d_{TR} \gg N\Delta d_T. \quad (15d)$$

The works in this paper hereinafter are based on the far-field approximations (12), (13) and (14). We propose an upper bound of the received power deviation due to the approximations in Appendix A. As seen, the received power deviation tends to zero as the far-field conditions (15) becomes more strict.

From (12) and (13), the phase changes of the signal, caused by the channel through IRS in free space, are essentially functions of the position of the IRS.

C. Problem Formulation

Most of the existing works, considering a fixed IRS, jointly optimized the beamforming vector \mathbf{v} , phase-shift matrix Θ to improve the received power, namely the information achievable rate. In this paper, the position of the IRS \mathbf{r} and the orientation of the IRS ξ are also under-determined variables, thus they can be utilized to further enhance the received power. Considering practical limitations, the joint optimization problem of IRS-assisted wireless communication is in the form of

$$\begin{aligned} (P1) : \quad & \max_{\mathbf{v}, \Theta, \mathbf{r}, \xi} P_r \\ \text{s. t.} \quad & \mathbf{v}^H \mathbf{v} \leq P_t \\ & \Theta \in \mathbb{B} \\ & \mathbf{r} \in \mathbb{S}_0 \cap \mathbb{S}_1 \cap \mathbb{S}_2. \end{aligned} \quad (16)$$

where \mathbb{S}_0 can be expressed as $d_{TI} \geq r_0 \cap d_{IR} \geq r_1$, r_0 and r_1 are the minimum distance to guarantee the far-field condition, respectively. \mathbb{S}_1 is the restriction that guarantees the EM to propagate from T to R through the IRS. \mathbb{S}_2 is the feasible area that the IRS can be fixed at. Herein, we denote the feasible set of Θ as \mathbb{B} here. Without loss of generality, we assume that the antennas in T and R are omni-directional¹.

The problem (P1) is a joint optimization of four variables, and it is challenging to solve directly. In the following, firstly, we deduce the optimal solutions of Θ and \mathbf{v} , assuming \mathbf{r} and ξ are fixed. This part belongs to the general beamforming design. Assuming \mathbf{r} is fixed, the optimal ξ is also derived. With the above solutions, the remaining problem becomes an unadulterated position optimizing problem to be solved. As a result, the globally optimal strategy for IRS-assisted wireless communication system is derived.

¹If we consider the directional antenna, only placing the IRS in the main lobe is meaningful. Let \mathbb{S}_3 denotes the area in the main lobe. Therefore, a new restriction $\mathbf{r} \in \mathbb{S}_3$ should be added to (P1).

III. OPTIMAL STRATEGY WITH A FIXED IRS

To decouple the solutions of Θ , \mathbf{v} , ξ with \mathbf{r} in problem (P1), we consider a fixed IRS in this section. The optimal Θ and \mathbf{v} are coupled with each other, but irrelevant to ξ . After deriving optimal Θ , \mathbf{v} and ξ , the effectiveness of the IRS to assist a wireless communication system shall be discussed.

A. Optimal Θ and \mathbf{v}

The solutions of Θ and \mathbf{v} for the fixed IRS can be obtained using the iteration method proposed in [7]. However, it's challenging to solve the joint optimization problem (P1). Herein, by exploiting the tightly coupled property of channel elements in the free space, we provide the analytic and optimal solutions of Θ and \mathbf{v} .

After expending matrix multiplication in (7) by specific entries written in (4)-(6), the following equation is obtained naturally.

$$P_r = \left\| \underbrace{a_{TI} a_{IR} \left[\sum_{q=1}^L \sum_{p=1}^N e^{j(\varphi_q + \theta_{IR,q} + \theta_{TI,q,p})} v_p \right]}_X + \mathbf{h}_{TR}^H \mathbf{v} \right\|^2. \quad (17)$$

The variables determined by the position of the IRS are coupled together in the exponent component (denoted as X) of (17). We deduce it to a form splitting the combination of the designable quantities (Θ and \mathbf{v}) and the variables. Extending X by (11)-(12) and the other similar formulas, we obtain

$$\begin{aligned} X &= \sum_{q=1}^L \left\{ e^{j(\varphi_q + \theta_{IR,q})} \left[\sum_{p=1}^N e^{j\theta_{TI,q,p}} v_p \right] \right\} \\ &\approx \underbrace{\left[\sum_{q=1}^L e^{j(\varphi_q + \frac{d_{IR,q} 2\pi}{\lambda} + \frac{d_{TI,0,q} 2\pi}{\lambda})} \right]}_A \underbrace{\left[\sum_{p=1}^N e^{j \frac{\Delta d_{T,p} \cos(\mu_{TI}) 2\pi}{\lambda}} v_p \right]}_B. \end{aligned} \quad (18)$$

For notation simplicity, we denote μ_{TI} as μ . Then, the term B in (18) can be written as vector production: $B = \mathbf{b}^H \mathbf{v}$. \mathbf{b}^H is defined as follows.

$$\mathbf{b}^H = \left[e^{j \frac{(N-1) \Delta d \cos(\mu) 2\pi}{\lambda}}, e^{j \frac{(N-3) \Delta d \cos(\mu) 2\pi}{\lambda}}, \dots, e^{j \frac{-(N-1) \Delta d \cos(\mu) 2\pi}{\lambda}} \right]^T. \quad (19)$$

The formula (17) is updated to the following formula

$$P_r = \left\| (a_{TI} a_{IR} A \mathbf{b}^H + \mathbf{h}_{TR}^H) \mathbf{v} \right\|^2. \quad (20)$$

For any given Θ , it is widely known that maximum-ratio transmission (MRT) is the optimal transmit beamforming to maximize the received power in [7], i.e.,

$$\mathbf{v}^* = \sqrt{P_t} \frac{(a_{TI} a_{IR} A \mathbf{b}^H + \mathbf{h}_{TR}^H)^H}{\|a_{TI} a_{IR} A \mathbf{b}^H + \mathbf{h}_{TR}^H\|}. \quad (21)$$

After using \mathbf{v}^* in (20), the received power can be rewritten as

$$P_r = P_t \left\| a_{TI} a_{IR} A \mathbf{b}^H + \mathbf{h}_{TR}^H \right\|^2, \quad (22)$$

where A is a variable controlled by the matrix Θ with maximum amplitude L and arbitrary designed phase. To obtain the

optimal received power, the phase shift of the q -th reflecting element is designed as

$$\begin{aligned} \varphi_q^* &= \left(\frac{O}{2|O|} - \frac{1}{2}\right)\pi - \frac{2\pi}{\lambda}(d_{IR} + d_{TI} - d_{TR}) \\ &\quad - (\sin\theta_t \cos\varphi_t + \sin\theta_r \cos\varphi_r)\left(m_q - \frac{M_I + 1}{2}\right)d_x \\ &\quad - (\sin\theta_t \sin\varphi_t + \sin\theta_r \sin\varphi_r)\left(n_q - \frac{N_I + 1}{2}\right)d_y, \\ O &\triangleq \frac{\text{sinc}\left(\frac{N\Delta d(\cos(\mu) - \cos(\mu_{TR}))2\pi}{2\lambda}\right)}{\text{sinc}\left(\frac{\Delta d(\cos(\mu) - \cos(\mu_{TR}))2\pi}{2\lambda}\right)}. \end{aligned} \quad (23)$$

Proof. See Appendix B. \square

According to the MRT, the decoupled analytic solutions of \mathbf{v}^* is given by

$$\mathbf{v}^* = \sqrt{P_t} \frac{(a_{TI}a_{IR}L e^{j[(\frac{O}{2|O|} - \frac{1}{2})\pi + \frac{d_{TR}2\pi}{\lambda}]} \mathbf{b}^H + \mathbf{h}_{TR}^H)^H}{\left\| a_{TI}a_{IR}L e^{j[(\frac{O}{2|O|} - \frac{1}{2})\pi + \frac{d_{TR}2\pi}{\lambda}]} \mathbf{b}^H + \mathbf{h}_{TR}^H \right\|}. \quad (24)$$

With the proposed closed-form beamforming and phase shifts, the optimal received power is given by

$$\begin{aligned} P_r &= NL^2(a_{TI}a_{IR})^2 P_t + Na_{TR}^2 P_t \\ &\quad + 2NL a_{TR} a_{TI} a_{IR} d_{TR} O P_t. \end{aligned} \quad (25)$$

B. Optimal Orientation of the IRS

Once the position of the IRS is determined, namely the reference point is fixed, the orientation of the IRS, denoted as ξ , can still be tuned to improve the received power via maximizing $F(\theta_t, \varphi_t)F(\theta_r, \varphi_r)$. The optimal value is denoted as F^* hereinafter. Due to large distance between the IRS and communication parties in far-field case, it's reasonable to treat all reflecting elements as the reference point when calculating F^* . The problem of tuning an IRS at a fixed point to reap the max power radiation gain, as illustrated in Fig. 2(b), is in the form of

$$\begin{aligned} \max_{\theta_t, \theta_r} \quad & \cos\theta_t \cos\theta_r \\ \text{s. t.} \quad & \theta_t \in \left(0, \frac{\pi}{2}\right) \\ & \theta_r \in \left(0, \frac{\pi}{2}\right) \\ & \theta_0 \leq \theta_t + \theta_r \leq 2\pi - \theta_0. \end{aligned} \quad (26)$$

When $\theta_t = \theta_r = \frac{\theta_0}{2}$, the objective function in (26) reaches the max value, denoted as F^* , which is given by

$$\begin{aligned} F^* &= \left(\cos^2 \frac{\theta_0}{2}\right)^k = \left(\frac{1}{2} \cos\theta_0 + \frac{1}{2}\right)^k \\ &= \left(\frac{d_{TI}^2 + d_{IR}^2 - d_{TR}^2}{4d_{TI}d_{IR}} + \frac{1}{2}\right)^k. \end{aligned} \quad (27)$$

From the above, we obtain the following theorem.

Theorem 1. *The optimal ξ is just to make the IRS perform specular reflection, that is, the incident signal is mainly reflected towards the mirror direction ($\theta_r = \theta_t$).*

It is worth mentioning that this result in the MISO system is consistent with the counterpart in the SISO system [26].

C. The Effectiveness of the IRS

The above analytic and near-optimal solutions bring convenience to discuss the max effectiveness brought by the IRS. Since focusing on the practical effectiveness of the IRS, we relate the physics and electromagnetic power model P'_r and the common simplified mathematical power P_r with a proportion factor α . According to [26], $\alpha = \frac{A_r}{2Z_0}$. The received power can be rewritten as $P'_r = \alpha P_r$.

In substance, the received signal is a sum of the signal from two link: direct link and IRS-assisted link. To analyse the effectiveness of IRS, we compare the maximum received power from the IRS-assisted link and direct link, denoted as $P'_r(TIR)^*$ and $P'_r(TR)^*$ respectively. The ratio between them can be expressed as

$$\frac{P'_r(TIR)^*}{P'_r(TR)^*} = \frac{P_r(TIR)^*}{P_r(TR)^*} = \frac{\alpha NL^2 \delta_{TIR}^2 P_t}{\alpha N \delta_{TR}^2 P_t} = \frac{LA_{IRS}GF^* \Gamma d_{TI}^{-2} d_{IR}^{-2}}{4\pi d_{TR}^2}, \quad (28)$$

where, A_{IRS} represents the surface area of the IRS. $A_{IRS} = LA_{element} = Ld_x d_y$.

From above, we summarize two extreme scenarios when adding a fabricated IRS to the free-space wireless communication system.

- 1) $LA_{IRS}GF^* \Gamma d_{TI}^{-2} d_{IR}^{-2} \ll 4\pi d_{TR}^2$. The direct link dominates the performance of wireless transmission in the free-space IRS-assisted wireless communication system. The assistance of a fabricated IRS is insignificant and unnecessary.
- 2) $LA_{IRS}GF^* \Gamma d_{TI}^{-2} d_{IR}^{-2} \gg 4\pi d_{TR}^2$. The IRS-assisted link dominates the performance of wireless transmission in the free-space IRS-assisted wireless communication system. The assistance of a fabricated IRS improves the user experience by a large margin.

Moreover, the assisted IRS is of the utmost importance if the direct path is blocked.

The received power proportion of two paths is not only related to the whole surface area of the IRS, but also the number of IRS elements. From the received power proportion formula (28), an IRS consisting of more reflecting elements is more effective. Only considering IRS-assisted link, via combining (7), (8) and the formula $A_r = \frac{G_r \lambda^2}{4\pi}$, the maximum received power is expressed as

$$\begin{aligned} P'_r(TIR)^* &= \alpha NL^2 \delta_{TIR}^2 P_t \\ &= \frac{NL^2 Z_0 G_t G_r G d_x d_y F(\theta_t, \varphi_t) F(\theta_r, \varphi_r) \Gamma^2 \lambda^2}{64\pi^3} P_t \\ &= \frac{\lambda^2}{d_x d_y} \frac{NA_{IRS}^2 Z_0 G_t G_r GF(\theta_t, \varphi_t) F(\theta_r, \varphi_r) \Gamma^2}{64\pi^3} P_t. \end{aligned} \quad (29)$$

As a tendency, millimeter-wave communication arouses wide concern in the field of wireless communication. However, the high-frequency millimeter wave is susceptible to the path length, resulting in a weak signal power at the receiver. This is a major difficulty reserving to be solved. When using a higher frequency wave, based on (29), we expound a conclusion to the design of the IRS without extending the area of the IRS as follows.

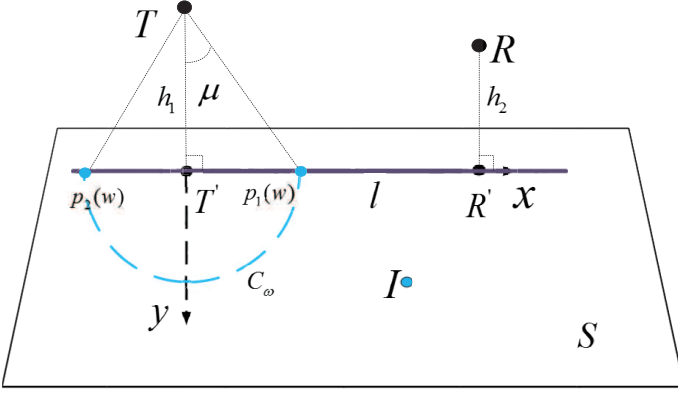


Fig. 3. Placing IRS in a normal plane and some notations.

Conclusion 1. To maintain the received power through IRS-assisted link with the increasing frequency of carrier wave, the side length of the reflecting element is in a fixed proportion to the carrier wavelength.

IV. OPTIMAL POSITION OF THE IRS

In this section, jointly with the optimal solutions of Θ , \mathbf{v} , ξ , we aim to find the optimal position of the IRS in problem (P1).

A. Optimal Position in Arbitrary Three-Dimensional Space

As the objective function to optimize the position of the IRS, the maximum received power (25) can be simplified as follows

$$\begin{aligned}
 F_{object} &= L \frac{\delta_{TIR}}{\sqrt{F^*}} (F^*)^{\frac{1}{2}} d_{TI}^{-1} d_{IR}^{-1} + 2\delta_{TR} d_{TR}^{-1} O \\
 &= L \frac{\delta_{TIR}}{\sqrt{F^*}} \underbrace{\left(\frac{d_{TI}^2 - d_{TR}^2}{4d_{TI}} d_{IR}^{-1} + \frac{1}{4d_{TI}} d_{IR} + \frac{1}{2} \right)^{\frac{k}{2}} d_{TI}^{-1} d_{IR}^{-1}}_{F_1} + \underbrace{2\delta_{TR} d_{TR}^{-1} O}_{F_2}.
 \end{aligned} \tag{30}$$

According to (8), $\frac{\delta_{TIR}}{\sqrt{F^*}}$ is a constant with no relationship of the position of the IRS. The position change of the IRS only impacts the value of terms d_{TI} , d_{IR} , O .

The position optimization question is formulated as

$$\begin{aligned}
 \text{(P2):} \quad & \max_{\mathbf{r}} F_{object} \\
 \text{s. t.} \quad & \mathbf{r} \in \mathbb{S},
 \end{aligned} \tag{31}$$

where $\mathbb{S} = \mathbb{S}_0 \cap \mathbb{S}_1 \cap \mathbb{S}_2$ represents the feasible space to place IRS. Due to the low-complexity of the objective function in (P2), exhaustive search method is recommended. However, for large three-dimensional space, this search method is still cumbersome. We'll study the property of optimal position in a two-dimensional plane, then extend it to arbitrarily three-dimensional space. According to the property, essential dimensionality reduction is achieved when searching in the feasible space.

It is known that a three-dimensional feasible space can be fully split into parallel two-dimensional subspaces. Then, the problem (P2) is replaced by many parallel subproblems, where the position of the IRS is an two-dimensional variable.

It is noted that the principle of splitting is flexible and has no influence to the final result. We propose a split method. Via doing so, the places are perpendicular to the ULA of the transmitter. The plane split by this method is named as normal plane. Firstly, not considering the constraints of placing IRS, we assume \mathbb{S} is an infinite large space. Then the parallel subproblems aim to optimize the position of IRS on an infinite large normal plane S . The system diagram of choosing the position of the IRS in the plane S is shown in Fig. 3. Adequately, we consider the $\frac{1}{2}$ plane of S due to the symmetry. Hereinafter, the plane S represents the half plane. The linear array direction pointing to the IRS side is the reference linear array direction. The line l denotes the line containing the projections of the reference points of T and R to plane S . The variable d_{IR} and ω ($\omega = \cos(\mu)$) can make the position of the IRS unique, as shown in Fig. 3. The optimal problem then is reformulated as:

$$\begin{aligned}
 & \max_{d_{IR}, \omega} F_{object} \\
 \text{s. t.} \quad & (d_{IR}, \omega) \in \mathbb{C} \\
 & d_{TI} = \frac{h_1}{\omega},
 \end{aligned} \tag{32}$$

where, \mathbb{C} represents possible union of d_{IR} and ω . For a given ω , the transportable trajectory of the IRS in plane S is a circle marked as C_ω , the value of F_2 in (30) is also fixed. After excavating the quasi-convex property of F_1 , the following theorems are obtained.

Theorem 2. If $k = 0$ in (10), then the optimal position on plane S is on the half of line l .

Proof. See Appendix C. \square

Theorem 3. If $k > 0$ in (10), the optimal position on area $S-D$ is on the line l . The area D is a area in the plane S satisfying $d_{TI} > d_{TR}$ as shown in Fig. 4.

Proof. See Appendix D. \square

Remark 1. When the h_1 becomes larger, the area D becomes smaller. If $h_1 > d_{TR}$, the area D doesn't exist. In far-field condition, the area D is usually negligible.

For the area mentioned in above theorems (S for $k = 0$ or $S-D$ for $k > 0$), (P2) can be simplified to the following one-dimension problem.

$$\begin{aligned}
 \text{(P3):} \quad & \max_{\omega} F_{object} \\
 \text{s. t.} \quad & d_{TI} = \frac{h_1}{\omega} \\
 & d_{IR} \in \mathbb{D} \\
 & \mathbb{D} \in \left\{ \sqrt{\left(d_{TR} - \frac{h_1}{|\tan(\arccos \omega)|} \right)^2 + h_2^2}, \sqrt{\left(d_{TR} + \frac{h_1}{|\tan(\arccos \omega)|} \right)^2 + h_2^2} \right\} \\
 & \omega \in [a, b].
 \end{aligned} \tag{33}$$

As the variable ω is in a small interval ($[a, b] \in (0, 1]$), it's not hard to go through the interval with a high precision.

Based on Appendices C and D, we put forward a useful corollary for an arbitrary two-dimensional area A feasible to place the IRS, illustrated in Fig. 4. It's applicable on the whole

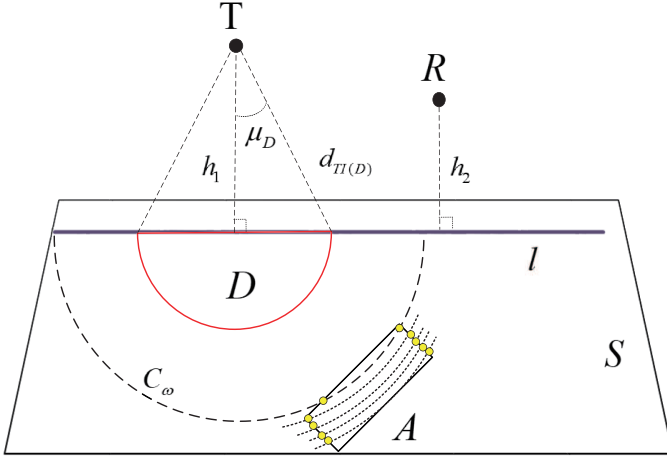


Fig. 4. Illustration of area D and corollary 1. D's borderline is a circle on where $d_{TI} = d_{TR}$. The yellow point denotes the optimal position of the IRS on the intersection of A and C_ω .

two-dimensional plane for $k = 0$ in (10) or a area except the area D for $k > 0$.

Corollary 1. *For an arbitrary feasible area on the whole plane S for $k = 0$ or $S-D$ for $k > 0$, separating from the line l, the optimal position of the IRS is on it's boundary.*

Finally, based on the fact that a three-dimensional space can be split to the normal planes fully, we extend above corollaries to the feasible space S. The following corollary is applicable on the whole three-dimensional space for $k = 0$ or a three-dimensional space except the circular column taking the area D as it's transversal surface for $k > 0$.

Corollary 2. *For an arbitrary space S in the whole three-dimensional space for $k = 0$ or the three-dimensional space except the circular column, taking the area D as it's transversal surface, for $k > 0$, separating from the plane consisting of the line containing the ULA and the line containing T and R, the optimal position of the IRS is always on the surface of S.*

B. Closed-form Optimal Position in A Special Case

In this subsection, we consider a special case that the signal from the direct path is extremely poor or the direct path is obstructed, only IRS-assisted link is meaningful. For the line parallel to the line from T to R as feasible space, a closed-form solution of the optimal position is presented. Only the signal reflected from the IRS is considered. The objective function in this case is reduced to the function F_1 in (30). Removing the irrelevant factors, the objective function to optimize the position of the IRS is simplified as

$$\cos\left(\frac{\theta_0}{2}\right)^k d_{TI}^{-1} d_{IR}^{-1}. \quad (34)$$

The meaning of (θ_0) is illustrated in Fig. 2(b). Using the formula $\frac{1}{2}d_{TR}h = \frac{1}{2}d_{TI}d_{IR}\sin\theta_0$, the objective function becomes

$$\frac{1}{d_{TR}h} \cos\left(\frac{\theta_0}{2}\right)^k \sin\theta_0. \quad (35)$$

The optimal solution denoted as θ_0^* is given as follows via taking the first-order derivative to θ_0 and setting it to zero

$$\theta_0^* = 2 \arctan \pm \frac{1}{k+1}. \quad (36)$$

Considering the advisable range of θ_0 , the expression of θ_0^* is reformulated as

$$\theta_0^* = \min\left\{2 \arctan \pm \frac{1}{k+1}, 2 \arctan \frac{d}{2h}\right\}. \quad (37)$$

In this situation, the optimal position of IRS is deduced from θ_0 , thus omitted here.

V. SIMULATIONS AND DISCUSSIONS

Numerical simulations about IRS-assisted wireless communication in free space have been conducted. The received power in simulations refers to physics and electromagnetic power P'_r defined in (7). Without loss of generality, we simulate a two-dimensional plane to place IRS. For a fixed IRS, the optimal strategy, including the proposed beamforming and phase shifts, the optimal orientation of IRS, is applied. The corresponding parameters are simplified in Table.II.

TABLE II
THE PARAMETERS OF IRS-ASSISTED WIRELESS COMMUNICATION IN SIMULATIONS

$N = 16, \lambda = 0.0286 \text{ m}, \Delta d = \frac{\lambda}{2},$
$d_x = d_y = 0.01 \text{ m}, L = 100 * 100,$
$G = 9.03 \text{ dB}, G_t = G_r = 21 \text{ dB}, \Gamma = 1,$
$k(in(10)) = 1, P_t = 0 \text{ dBm}.$

The distance between T and R is 200 m. The complement angle of DOA for R is on the perpendicular to the ULA (for convenience of simulation but not necessary). According to [31], the boundary of far-field and near field of the IRS is about 71.4 m ($\frac{2Ld_x d_y}{\lambda}$). However, from experiments in [26], the redefined boundary is about 28.77 m.² The IRS is freely placed on a normal plane S, which is perpendicular to the ULA. The coordinate origin is selected as the projection of T on plane S. Without loss of generality, $h_1 = h_2 = h$.

Fig. 5 demonstrates the curves of the received power when moving the IRS's reference point on the plane via traversal grid. As seen, the power is near a constant when the IRS is very far, for only direct path taking into account. As seen, the optimal solution is near the projection of R, especially when the distance between transmitter/receiver and the plane S is small. Through simulation, the best performance is just on the half of line l, in accordance with theorem. 3.

In more details, the received power when moving the IRS on the half line of l is presented in Fig. 6. At optimal position

²It is worth mention that this result consists with the conclusion that far-field can be relax to the "far" condition, which is also illustrated in [25].

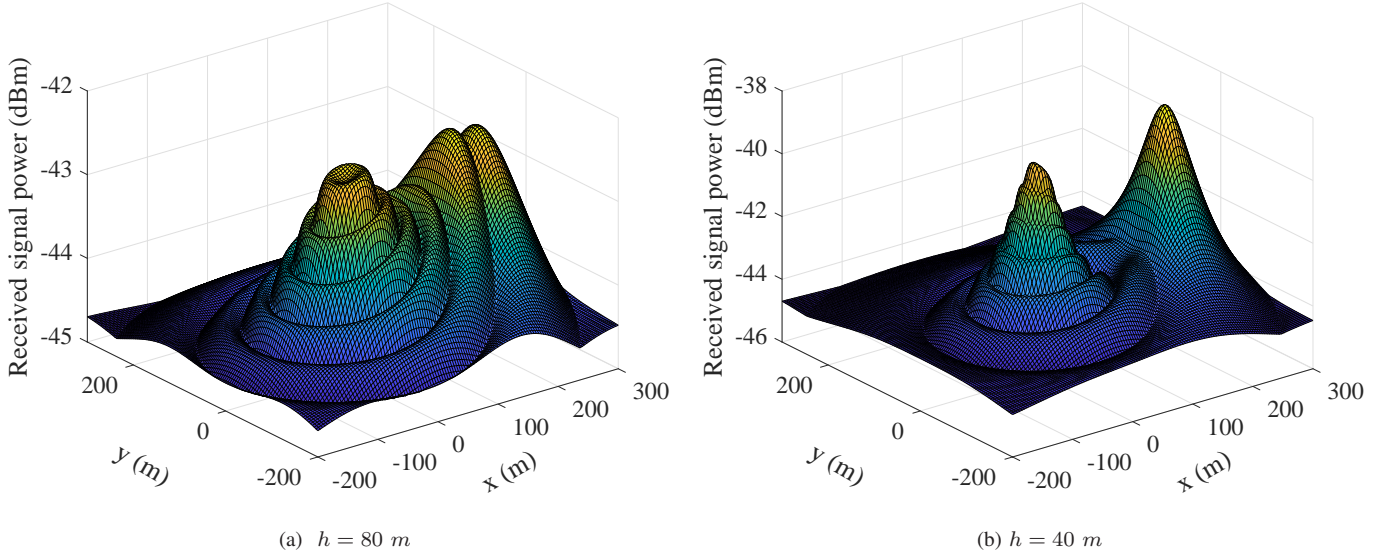


Fig. 5. The received power versus the position of the IRS

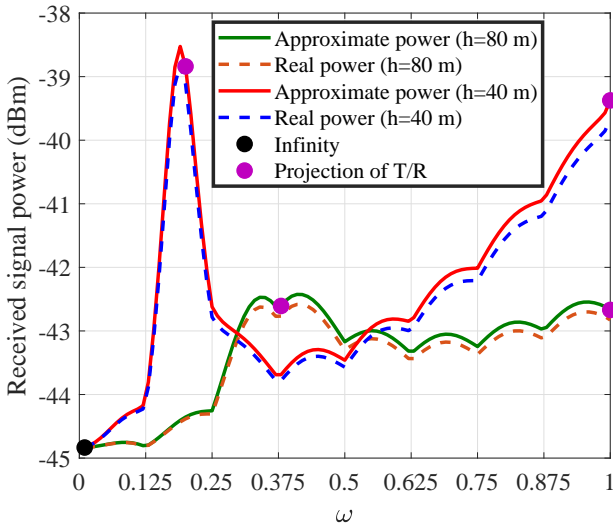


Fig. 6. The received signal power versus the position of the IRS on the half of line l (case 1)

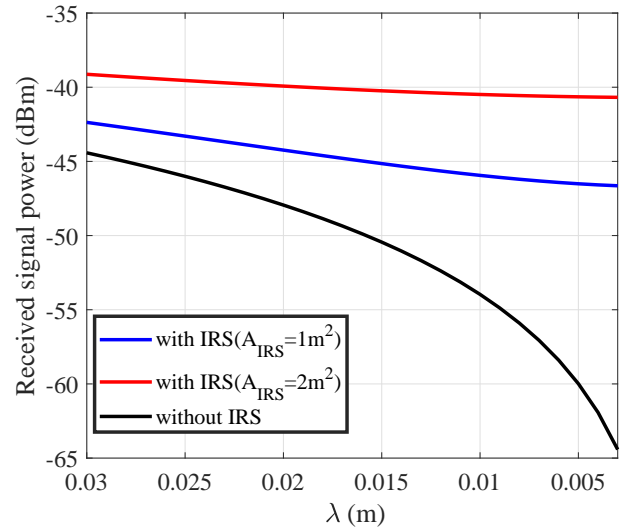


Fig. 7. The received signal power versus the carrier wave length

and using optimal placement, adding an IRS brings about 2 dB gain of the received power compared to without IRS (refer to the infinity point) when $h = 80 \text{ m}$. The improvement by the IRS is more obvious for $h = 40 \text{ m}$, the gain of the received power by placing the assisted IRS becomes 6.3 dB . Besides, while using the same strategy, the received power when the element in the channel matrix is original (called real power) is considered. This is to say not using any approximation from far-field condition mentioned in this paper. It's interesting that even for $h = 40 \text{ m}$ which is not exactly satisfied far-field condition, the real power still coincides well with the ideal power. This is mainly due to the small area of the IRS (1 m^2). From the simulation result, position optimization is

indispensable to the received power.

Fig. 7 plots the received power when varying carrier wavelength. The manufactured IRS in the figure satisfies the condition in *conclusion 1*. The considered parameters are: $h = 80 \text{ m}$, $k = 1$ and $dx * dy = \frac{1}{3}\lambda^2$ and the IRS is fixed at the project of R on plane S. As the wavelength decreases, the max received power from direct link decays largely but the max received power from IRS-assisted link stays the same. In another word, IRS is absolutely advantageous to assist free-space millimeter wave wireless communication system.

VI. CONCLUSION

In this paper, comprehensive optimization of incorporating an IRS to MISO wireless communication (the transmitter is equipped with an ULA) in free space has been considered from electromagnetic and physics perspective. The closed-form solution of transmitter's beamforming and phase shifts have been proposed. Considering the general power radiation pattern, we have proved that the optimal orientation of the IRS is just to satisfy specular reflection. United with the above contributions, the position of the IRS for global optimization has been studied. For most three-dimensional space as the feasible space of placing the IRS, a substantial dimensionality reduction theory was provided, reducing the complexity of search largely. From the numerical results, the proposed closed-form solutions of beamforming and phase shifts are also near-optimal. The results indicated that adding an IRS to wireless communication is remarkable and position optimization improves the performance significantly. Moreover, under the limit of total area of IRS, increasing the number of reflecting elements is an effective approach to countervail the deteriorating path loss in millimeter wave communication.

APPENDIX A

AN UPPER BOUND OF RECEIVED POWER DEVIATION FROM FAR-FIELD APPROXIMATIONS

In this section, we aim to find an upper bound of the received power deviation caused by far-field approximations. Let{ $\tilde{\cdot}$ } operator denote the value caused by far-field approximations. Let{ $\dot{\cdot}$ } operator denote the real value in the free-space communication system in free-space.

$$\begin{aligned}
\dot{P}_r &= |(\dot{\mathbf{h}}_{IR}^H \Theta \dot{\mathbf{H}}_{TI}^H + \dot{\mathbf{h}}_{TR}^H) \mathbf{v}|^2 \leq \left\| \dot{\mathbf{h}}_{IR}^H \Theta \dot{\mathbf{H}}_{TI}^H + \dot{\mathbf{h}}_{TR}^H \right\|^2 \\
&= \left\| \theta(\tilde{\mathbf{H}}_{TIR}^H + \Delta \tilde{\mathbf{H}}_{TI}^H) + \tilde{\mathbf{h}}_{TR}^H + \Delta \tilde{\mathbf{h}}_{TR} \right\|^2 \\
&= \tilde{P}_r + 2\sqrt{\tilde{P}_r} \left\| \theta \Delta \mathbf{H}_{TIR}^H + \Delta \mathbf{h}_{TR} \right\| \\
&\quad + \underbrace{\left\| \theta \Delta \mathbf{H}_{TIR}^H + \Delta \mathbf{h}_{TR} \right\|^2}_{\Delta P_r} \tag{38}
\end{aligned}$$

where $\tilde{\mathbf{H}}_{TIR} = \text{diag}(\tilde{\mathbf{h}}_{IR}^H) \tilde{\mathbf{H}}_{TI}^H$, $\dot{\mathbf{H}}_{TIR} = \text{diag}(\dot{\mathbf{h}}_{IR}^H) \dot{\mathbf{H}}_{TI}^H$, $\Delta \mathbf{H}_{TIR} = \tilde{\mathbf{H}}_{TIR} - \dot{\mathbf{H}}_{TIR}$ and $\Delta \mathbf{h}_{TR} = \tilde{\mathbf{h}}_{TR} - \dot{\mathbf{h}}_{TR}$.

The upper bound of ΔP_r is expressed as follows.

$$\begin{aligned}
\sqrt{\Delta P_r} &\leq \left\| \theta \Delta \mathbf{H}_{TIR}^H \right\| + \left\| \Delta \mathbf{h}_{TR} \right\| \\
&\leq \left\| \theta \right\| \left\| \Delta \mathbf{H}_{TIR}^H \right\| + \left\| \Delta \mathbf{h}_{TR} \right\| \\
&= \sqrt{L} \left\| \Delta \mathbf{H}_{TIR}^H \right\| + \left\| \Delta \mathbf{h}_{TR} \right\| \\
&\leq \sqrt{L} \left\| \Delta \mathbf{H}_{TIR}^H \right\|_F + \left\| \Delta \mathbf{h}_{TR} \right\|. \tag{39}
\end{aligned}$$

The 2-norm of the channel deviation in free space can be written as

$$\begin{aligned}
&\left\| \Delta \mathbf{h}_{TR} \right\| \\
&= \sqrt{\sum_{p=1}^N |e^{j\dot{\theta}_{TR,p}} - e^{j\tilde{\theta}_{TR,p}}|^2} \\
&= a_{TR} \sqrt{\sum_{p=1}^N |e^{j(\tilde{\theta}_{TR,p} + \frac{\Delta\theta_{TR,p}}{2}) + \frac{\Delta\theta_{TR,p}}{2}} - e^{j(\tilde{\theta}_{TR,p} + \frac{\Delta\theta_{TR,p}}{2}) - \frac{\Delta\theta_{TR,p}}{2}}|^2} \\
&= a_{TR} \sqrt{\sum_{p=1}^N 4 \sin^2 \frac{\Delta\theta_{TR,p}}{2}} \\
&= 2a_{TR} \sqrt{\sum_{p=1}^N \sin^2 \frac{\pi \Delta d_{TR,p}}{\lambda}} \tag{40}
\end{aligned}$$

where $\Delta\theta_{TR,p} = \dot{\theta}_{TR,p} - \tilde{\theta}_{TR,p}$ and $\Delta d_{TR,p} = \dot{d}_{TR,p} - \tilde{d}_{TR,p}$. $\Delta d_{TR,p}$ accounts for the far-field distance deviation from the p -th antenna of the transmitter to the receiver. Similarly,

$$\begin{aligned}
&\left\| \Delta \mathbf{H}_{TIR}^H \right\|_F \\
&= a_{TIR} \sqrt{\sum_{p=1}^N \sum_{q=1}^L |e^{j(\dot{\theta}_{TI,p,q} + \dot{\theta}_{IR,q})} - e^{j(\tilde{\theta}_{TI,p,q} + \tilde{\theta}_{IR,q})}|^2} \\
&= 2a_{TI} a_{IR} \sqrt{\sum_{p=1}^N \sum_{q=1}^L \sin^2 \frac{\pi(\Delta d_{TI,p,q} + \Delta d_{IR,q})}{\lambda}} \tag{41}
\end{aligned}$$

where $\Delta d_{TI,p,q} = \dot{d}_{TI,p,q} - \tilde{d}_{TI,p,q}$. $\Delta d_{IR,q} = \dot{d}_{IR,q} - \tilde{d}_{IR,q}$. $\Delta d_{TI,p,q}$ accounts for the far-field distance deviation from the p -th antenna of the transmitter to the q -th element of the IRS while $\Delta d_{IR,q}$ accounts for the far-field distance deviation from the q -th antenna of the IRS to the receiver.

Since the last two terms in last equation of (38) are positive, an upper bound of received power deviation is expressed as follows.

$$\begin{aligned}
&|\dot{P}_r - P_r| \\
&\leq 2\sqrt{\Delta P_r} \sqrt{P_r} + \Delta P_r \\
&= 4a_{TI} a_{IR} \sqrt{L} \sqrt{\sum_{p=1}^N \sum_{q=1}^L \sin^2 \frac{\pi(\Delta d_{TI,p,q} + \Delta d_{IR,q})}{\lambda}} + a_{TR} \sqrt{\sum_{p=1}^N \sin^2 \frac{\pi \Delta d_{TR,p}}{\lambda}} \sqrt{P_r} \\
&\quad + 4(a_{TI} a_{IR} \sqrt{L} \sqrt{\sum_{p=1}^N \sum_{q=1}^L \sin^2 \frac{\pi(\Delta d_{TI,p,q} + \Delta d_{IR,q})}{\lambda}} + a_{TR} \sqrt{\sum_{p=1}^N \sin^2 \frac{\pi \Delta d_{TR,p}}{\lambda}})^2. \tag{42}
\end{aligned}$$

It is known that, as $\frac{d_{TI}}{N\Delta d_T}$, $\frac{d_{TI}}{L\sqrt{d_x^2 + d_y^2}} \rightarrow \infty$, $\Delta d_{TI,p,q} \rightarrow 0$. As $\frac{d_{TR}}{N\Delta d_T} \rightarrow \infty$, $\Delta d_{TR,p} \rightarrow 0$. As $\frac{d_{IR}}{L\sqrt{d_x^2 + d_y^2}} \rightarrow \infty$, $\Delta d_{IR,q} \rightarrow 0$. As a conclusion, as $\frac{d_{TI}}{N\Delta d_T}$, $\frac{d_{TR}}{L\sqrt{d_x^2 + d_y^2}}$, $\frac{d_{TR}}{N\Delta d_T}$, $\frac{d_{IR}}{L\sqrt{d_x^2 + d_y^2}} \rightarrow \infty$, $|\dot{P}_r - P_r| \rightarrow 0$.

APPENDIX B OPTIMAL PHASE SHIFTS

$$\begin{aligned}
\frac{P_r}{P_t} &= \left\| a_{TI} a_{IR} \mathbf{A} \mathbf{b}^H + \mathbf{h}_{TR}^H \right\|^2 \\
&= \left\| a_{TI} a_{IR} \underbrace{\mathbf{A} e^{-j\frac{d_{TR} 2\pi}{\lambda}}}_{\mathbf{A}'} \mathbf{b}^H + e^{-j\frac{d_{TR} 2\pi}{\lambda}} \mathbf{h}_{TR}^H \right\|^2. \tag{43}
\end{aligned}$$

We express A' as Me^{jx} ($M \subset [0 \ L], x \subset [0 \ 2\pi]$) and

$$Me^{jx} = \sum_{q=1}^L \underbrace{e^{j(\varphi_q + \frac{(d_{IR,q} + d_{TI,0,q} - d_{TR})2\pi}{\lambda})}}_{A'_q}. \quad (44)$$

Substitute (19) into (43) with new formulation of A' .

$$\begin{aligned} \frac{P_r}{P_t} &= \sum_{p=1}^N |a_{TI}a_{IR}ME_1(p) + a_{TR}E_2(p)|^2 \\ &= N(a_{TI}a_{IR}M)^2 + Na_{TR}^2 + 2Ma_{TI}a_{IR}a_{TR}E_3, \end{aligned} \quad (45)$$

where,

$$\begin{aligned} E_1(p) &= e^{jx-j\frac{[p-\frac{(N+1)}{2}]\Delta d \cos(\mu)2\pi}{\lambda}}, \\ E_2(p) &= e^{j\frac{-[p-\frac{(N+1)}{2}]\Delta d \cos(\mu_{TR})2\pi}{\lambda}}, \\ E_3 &= \sum_{p=1}^N \underbrace{\cos(x - \underbrace{[p - \frac{(\frac{N+1}{2}\Delta d(\cos(\mu) - \cos(\mu_{TR}))2\pi}{\lambda})]}_{K_p})}_{K}. \end{aligned} \quad (46)$$

wherein, μ_{TR} denotes the DOA of the receiver.

$$\begin{aligned} K &= \cos(x) \sum_{p=1}^N \cos(K_p) + j \sin(x) \sum_{p=1}^N \sin(K_p) \\ &\stackrel{a}{=} \cos(x) \sum_{p=1}^N \cos(K_p) \\ &\stackrel{b}{=} \cos(x) \sum_{p=1}^N e^{jK_p} \\ &\stackrel{c}{=} N \cos(x) \underbrace{\frac{\text{sinc}(\frac{N\Delta d(\cos(\mu) - \cos(\mu_{TR}))2\pi}{2\lambda})}{\text{sinc}(\frac{\Delta d(\cos(\mu) - \cos(\mu_{TR}))2\pi}{2\lambda})}}_O, \end{aligned} \quad (47)$$

where (a) and (b) are due to the symmetry of sin function and (c) results from e^{jK_p} ($p = 1 : N$) is a geometric progression. Simple to verify that when $M = L$ and $\cos(x) = \frac{O}{|O|}$, P_r gets it's max value. A' can achieve this requirement if and only if

$$\begin{aligned} \varphi_q^* &= \left(\frac{O}{2|O|} - \frac{1}{2}\right)\pi - \frac{(d_{IR,q} + d_{TI,0,q} - d_{TR})2\pi}{\lambda} \\ &= \left(\frac{O}{2|O|} - \frac{1}{2}\right)\pi - \frac{2\pi}{\lambda}(d_{IR} + d_{TI} - d_{TR} - \\ &\quad - (\sin \theta_t \cos \varphi_t + \sin \theta_r \cos \varphi_r)(m_q - \frac{M_I + 1}{2})d_x \\ &\quad - (\sin \theta_t \sin \varphi_t + \sin \theta_r \sin \varphi_r)(n_q - \frac{N_I + 1}{2})d_y) \end{aligned} \quad (48)$$

APPENDIX C PROOF OF Theorem. 2

For any fixed ω , the orbit of feasible position is a circle C_ω in plane S. If ω is fixed, the value of F_2 is fixed and d_{TI} is also certain. $F_1(d_{IR})$ decreases from $p_2(\omega)$ to $p_1(\omega)$ along C_ω . $F_1(d_{IR})$ is a decreasing function to d_{IR} , the value of F_1 is max at point $p_1(\omega)$. Therefore, for a arbitrarily point not on the line l, there must exist a point at which the object function

is bigger. Therefore on the plane S, optimal position is must on the half of the line l.

APPENDIX D PROOF OF Theorem. 3

If in an area, for any fixed ω , $F_1(d_{IR})$ is a quasiconvex function to d_{IR} . Similar to Appendix C, and based on the basic property of quasiconvex function (Section 3.4.2 in [32]), the optimal position is in line l in the area. Notice that it is the line l, not the half line l due to monotonicity. We'll proof in the area $S - D$, $F_1(d_{IR})$ is a quasiconvex function.

For a more convenient expression, we simplify d_{IR} as x . Then the function $F_1(x)$ can be written as

$$F_1(x) = cx^{-1} \underbrace{(ax^{-1} + bx + \frac{1}{2})^{\frac{k}{2}}}_{f(x)} \quad x > 0. \quad (49)$$

Wherein, the constant $a = \frac{d_{TI}^2 - d_{TR}^2}{4d_{TI}}$, $b > 0$, $c = L \frac{\delta_{TIR}}{\sqrt{F^*}} > 0$, $k > 0$ and $0 < f(x) < 1$, deducing from (27). So $S - D$ is the area where $a > 0$. To proof the theorem is equal to proof $F_1(x)$ is a quasiconvex function for $a > 0$.

The derivation of $F_1(x)$, denoted as $F'_1(x)$ is given by

$$F'_1(x) = -cf(x)^{\frac{k}{2}}x^{-2} + \frac{k}{2}x^{-1}f(x)^{(\frac{k}{2}-1)}f'(x), \quad (50)$$

where,

$$f'(x) = (-ax^{-2} + b). \quad (51)$$

proof ($0 < k \leq 2$):

$$F'_1(x) = c[f(x)^{(\frac{k}{2}-1)}x^{-2}] \underbrace{(-f(x) + \frac{k}{2}xf'(x))}_{g(x)}. \quad (52)$$

Because $0 < f(x)$, $g(x)$ determines whether $F'_1(x)$ is positive or negative.

$$\begin{aligned} g(x) &= -(ax^{-1} + bx + \frac{1}{2}) + \frac{k}{2}(-ax^{-1} + bx) \\ &= -(\frac{k}{2} + 1)ax^{-1} + (\frac{k}{2} - 1)bx - \frac{1}{2} \\ &< 0. \end{aligned} \quad (53)$$

So, $F_1(x)$ is a quasiconvex (quasilinear) function for $a > 0$, $0 < k \leq 2$. ■

proof ($k \geq 2$): The condition for $F'_1(x) = 0$ is

$$f(x) = \frac{k}{2}xf'(x). \quad (54)$$

If the solution doesn't exists, then $F_1(x)$ is a quasiconvex (quasilinear) function. If it exists, (54) implies $f'(x) > 0$ when it holds.

$$\begin{aligned} \frac{F''_1(x)}{c} &= (x^{-3}f(x)^{\frac{k}{2}-2})(-\frac{k}{2}xf(x)f'(x) + 2f(x)^2 \\ &\quad - \frac{k}{2}xf(x)f'(x) + \frac{k}{2}(\frac{k}{2} - 1)x^2f'(x)^2 + \frac{k}{2}x^2f(x)f''(x)) \\ &\triangleq (x^{-3}f(x)^{\frac{k}{2}-2})h(x), \end{aligned} \quad (55)$$

where,

$$f''(x) = 2ax^{-3}. \quad (56)$$

Due to $f(x) > 0, c > 0$, whether $F_1''(x)$ is negative or positive is determined by $h(x)$.

$$\begin{aligned} h(x) &= f(x) \underbrace{\left[-\frac{k}{2}xf'(x) + f(x)\right]}_Q + f(x)^2 \\ &\quad - \frac{k}{2}xf'(x) \underbrace{\left[f(x) - \frac{k}{2}xf'(x)\right]}_Q - \frac{k}{2}x^2f'(x)^2 + \frac{k}{2}x^2f(x)f''(x) \\ &\stackrel{a}{=} f(x)^2 - \frac{k}{2}x^2f'(x)^2 + \frac{k}{2}x^2f(x)f''(x) \\ &\stackrel{b}{=} \left(\frac{k^2}{4} - \frac{k}{2}\right)x^2f'(x)^2 + kax^{-1}f(x) \\ &> 0. \end{aligned} \quad (57)$$

Wherein, (a) is due to $Q = 0$ when (54) holds. (b) results from the substitution of (54) and (56). Therefore, $F_1(x)$ is a quasiconvex function for $a > 0, k > 2$. ■

REFERENCES

- [1] T. J. Cui, M. Q. Qi, X. Wan, J. Zhao, and Q. Cheng, "Coding metamaterials, digital metamaterials and programmable metamaterials," *Light, Sci. Appl.*, vol. 3, no. 10, p. e218, 2014.
- [2] Huanhuan, Yang, Xiangyu, Cao, Fan, Jun, Gao, Shenheng, Xu, and M. and, "A programmable metasurface with dynamic polarization, scattering and focusing control," *Sci. Rep.*, vol. 6, no. 1, p. 129, 2016.
- [3] C. Liaskos, S. Nie, A. Tsioliaridou, A. Pitsillides, S. Ioannidis, and I. Akyildiz, "A new wireless communication paradigm through software-controlled metasurfaces," *IEEE Commun. Mag.*, vol. 56, no. 9, pp. 162–169, 2018.
- [4] Q. Wu and R. Zhang, "Towards smart and reconfigurable environment: Intelligent reflecting surface aided wireless network?" *IEEE Commun. Mag.*, vol. 58, no. 1, pp. 106–112, January 2020.
- [5] M. Di Renzo, K. Ntontin, J. Song, F. H. Danufane, X. Qian, F. Lazarakis, J. De Rosny, D.-T. Phan-Huy, O. Simeone, R. Zhang, M. Debbah, G. Lerosey, M. Fink, S. Tretyakov, and S. Shamai, "Reconfigurable intelligent surfaces vs. relaying: Differences, similarities, and performance comparison," *IEEE J. Select. Areas Commun.*, vol. 1, pp. 798–807, 2020.
- [6] M. Cui, G. Zhang, and R. Zhang, "Secure wireless communication via intelligent reflecting surface," *IEEE Wireless Commun. Lett.*, vol. 8, no. 5, pp. 1410–1414, 2019.
- [7] Q. Wu and R. Zhang, "Intelligent reflecting surface enhanced wireless network: Joint active and passive beamforming design," in *IEEE Global Communications Conference, GLOBECOM 2018, Abu Dhabi, United Arab Emirates, December 9-13, 2018*, 2018, pp. 1–6.
- [8] X. Yu, D. Xu, and R. Schober, "MISO wireless communication systems via intelligent reflecting surfaces : (invited paper)," in *2019 IEEE/CIC International Conference on Communications in China (ICCC)*, 2019, pp. 735–740.
- [9] W. Shi, X. Zhou, L. Jia, Y. Wu, F. Shu, and J. Wang, "Enhanced secure wireless information and power transfer via intelligent reflecting surface," *IEEE Commun. Lett.*, vol. 25, no. 4, pp. 1084–1088, 2021.
- [10] Y. Han, W. Tang, S. Jin, C. Wen, and X. Ma, "Large intelligent surface-assisted wireless communication exploiting statistical CSI," *IEEE Trans. Veh. Technol.*, vol. 68, no. 8, pp. 8238–8242, 2019.
- [11] C. Pan, H. Ren, K. Wang, M. ElKashlan, A. Nallanathan, J. Wang, and L. Hanzo, "Intelligent reflecting surface aided MIMO broadcasting for simultaneous wireless information and power transfer," *IEEE J. Sel. Areas Commun.*, vol. 38, no. 8, pp. 1719–1734, 2020.
- [12] C. Pan, H. Ren, K. Wang, W. Xu, M. ElKashlan, A. Nallanathan, and L. Hanzo, "Multicell MIMO communications relying on intelligent reflecting surfaces," *IEEE Trans. Wireless Commun.*, vol. 19, no. 8, pp. 5218–5233, 2020.
- [13] W. Shi, J. Li, G. Xia, Y. Wang, X. Zhou, Y. Zhang, and F. Shu, "Secure multigroup multicast communication systems via intelligent reflecting surface," *China Commun.*, vol. 18, no. 3, pp. 39–51, 2021.
- [14] J. Ye, S. Guo, and M.-S. Alouini, "Joint reflecting and precoding designs for ser minimization in reconfigurable intelligent surfaces assisted mimo systems," *IEEE Trans. Wireless Commun.*, vol. 19, no. 8, pp. 5561–5574, 2020.
- [15] H. Shen, W. Xu, S. Gong, Z. He, and C. Zhao, "Secrecy rate maximization for intelligent reflecting surface assisted multi-antenna communications," *IEEE Commun. Lett.*, vol. 23, no. 9, pp. 1488–1492, 2019.
- [16] X. Zhou, S. Yan, Q. Wu, F. Shu, and D. W. K. Ng, "Intelligent reflecting surface (IRS)-aided covert wireless communication with delay constraint," *CoRR*, vol. abs/2011.03726, 2020. [Online]. Available: <https://arxiv.org/abs/2011.03726>
- [17] F. Shu, J. Li, M. Huang, W. Shi, Y. Teng, J. Li, Y. Wu, and J. Wang, "Enhanced secrecy rate maximization for directional modulation networks via IRS," *CoRR*, vol. abs/2008.05067, 2020. [Online]. Available: <https://arxiv.org/abs/2008.05067>
- [18] M. Jung, W. Saad, Y. Jang, G. Kong, and S. Choi, "Reliability analysis of large intelligent surfaces (LISs): Rate distribution and outage probability," *IEEE Wireless Commun. Lett.*, vol. 8, no. 6, pp. 1662–1666, 2019.
- [19] A. Taha, M. Alrabeiah, and A. Alkhateeb, "Enabling large intelligent surfaces with compressive sensing and deep learning," *IEEE Access.*, pp. 1–1, 2021.
- [20] Z. He and X. Yuan, "Cascaded channel estimation for large intelligent metasurface assisted massive MIMO," *IEEE Wireless Commun. Lett.*, vol. 9, no. 2, pp. 210–214, 2020.
- [21] Q. Wu and R. Zhang, "Beamforming optimization for wireless network aided by intelligent reflecting surface with discrete phase shifts," *IEEE Trans. Commun.*, vol. 68, no. 3, pp. 1838–1851, 2020.
- [22] S. Abeywickrama, R. Zhang, Q. Wu, and C. Yuen, "Intelligent reflecting surface: Practical phase shift model and beamforming optimization," *IEEE Trans. Commun.*, vol. 68, no. 9, pp. 5849–5863, 2020.
- [23] S. Guo, S. Lv, H. Zhang, J. Ye, and P. Zhang, "Reflecting modulation," *IEEE J. Select. Areas Commun.*, vol. 38, no. 11, pp. 2548–2561, 2020.
- [24] Ö. Özdogan, E. Björnson, and E. G. Larsson, "Intelligent reflecting surfaces: Physics, propagation, and pathloss modeling," *IEEE Wireless Commun. Lett.*, vol. 9, no. 5, pp. 581–585, 2020.
- [25] S. W. Ellingson, "Path loss in reconfigurable intelligent surface-enabled channels," *CoRR*, vol. abs/1912.06759, 2019. [Online]. Available: <http://arxiv.org/abs/1912.06759>
- [26] W. Tang, M. Z. Chen, X. Chen, J. Y. Dai, Y. Han, M. Di Renzo, Y. Zeng, S. Jin, Q. Cheng, and T. J. Cui, "Wireless communications with reconfigurable intelligent surface: Path loss modeling and experimental measurement," *IEEE Trans. Wireless Commun.*, vol. 20, no. 1, pp. 421–439, 2021.
- [27] W. L. Stutzman and G. A. Thiele, *Antenna Theory and Design*. New York : J. Wiley., 1997.
- [28] A. Goldsmith, *Wireless Communications*. Cambridge University Press, 2005.
- [29] A. Sayeed and J. Brady, "Beamspace MIMO for high-dimensional multiuser communication at millimeter-wave frequencies," in *2013 IEEE Global Communications Conference (GLOBECOM)*, 2013, pp. 3679–3684.
- [30] A. M. Sayeed and N. Behdad, "Continuous aperture phased MIMO: A new architecture for optimum line-of-sight links," in *2011 IEEE International Symposium on Antennas and Propagation (APSURSI)*, 2011, pp. 293–296.
- [31] Y. Huang and K. Boyle, "Antennas: From theory to practice," *Chichester, U.K.: Wiley.*, 2008.
- [32] S. Boyd and L. Vandenberghe, *Convex Optimization*. Cambridge, U.K.: Cambridge Univ. Press, 2004.